



## Diagnosis of Periprosthetic Hip Joint Infection Using MRI with Metal Artifact Reduction at 1.5 T

Galley, Julien ; Sutter, Reto ; Stern, Christoph ; Filli, Lukas ; Rahm, Stefan ; Pfirrmann, Christian W A

**Abstract:** Background MRI with metal artifact reduction has gained importance in assessment of pain with total hip arthroplasty (THA). However, its role in diagnosis of periprosthetic joint infection (PJI) has not been well defined. Purpose To evaluate findings of PJI after THA and to determine the diagnostic performance of 1.5-T MRI with metal artifact reduction. Materials and Methods Dedicated compressed sensing-based slice encoding for metal artifact correction 1.5-T MRI examinations (from January 2015 to April 2018) in patients with THA PJI (infection group) and noninfected THA (control group) were retrospectively evaluated by two musculoskeletal radiologists. Fisher exact test was used to compare the groups. Sensitivity, specificity, and accuracy were evaluated for each finding. Interobserver reliability was assessed with  $\kappa$  statistics. Results Forty patients (mean age, 69 years  $\pm$  11 [standard deviation]; 26 men) in the infection group and 100 patients (mean age, 67 years  $\pm$  11; 42 men) in the control group were evaluated. Periosteal reaction, capsule edema, and intramuscular edema differed between the two groups ( $P < .001$  for each finding). Periosteal reaction was found in 31 of 40 patients with infection and 10 of 100 participants in the control group (sensitivity, 78%; specificity, 90%; accuracy, 86%); capsule edema was found in 33 of 40 (infection group) and five of 100 (control group) (sensitivity, 83%; specificity, 95%; accuracy, 91%); and intramuscular edema was found in 38 of 40 (infection group) and 14 of 100 (control group) (sensitivity, 95%; specificity, 86%; accuracy, 89%). Interobserver agreement was almost perfect, with  $\kappa$  values between 0.88 and 0.92. No difference between the two groups was found regarding the presence of osteolysis (infection group, 23 of 40; control group, 60 of 100), bone marrow edema (39 of 40 vs 87 of 100), effusion (20 of 40 vs 26 of 100), abductor tendon lesion (22 of 40 vs 62 of 100), or bursitis (14 of 40 vs 34 of 100) ( $P > .05$  for each finding). Conclusion The presence of periosteal reaction, capsule edema, and intramuscular edema after total hip arthroplasty at 1.5-T MRI with metal artifact reduction had a high accuracy in evaluation of periprosthetic joint infection. © RSNA, 2020 Online supplemental material is available for this article. See also the editorial by Zanetti in this issue.

DOI: <https://doi.org/10.1148/radiol.2020191901>

Posted at the Zurich Open Repository and Archive, University of Zurich

ZORA URL: <https://doi.org/10.5167/uzh-199384>

Journal Article

Published Version



The following work is licensed under a Creative Commons: Attribution-NonCommercial-NoDerivatives 4.0 International (CC BY-NC-ND 4.0) License.

Originally published at:

Galley, Julien; Sutter, Reto; Stern, Christoph; Filli, Lukas; Rahm, Stefan; Pfirrmann, Christian W A (2020). Diagnosis of Periprosthetic Hip Joint Infection Using MRI with Metal Artifact Reduction at 1.5 T. *Radiology*, 296(1):98-108.

DOI: <https://doi.org/10.1148/radiol.2020191901>


# Diagnosis of Periprosthetic Hip Joint Infection Using MRI with Metal Artifact Reduction at 1.5 T

Julien Galley, MD • Reto Sutter, MD • Christoph Stern, MD • Lukas Filli, MD • Stefan Rahm, MD • Christian W. A. Pfirrmann, MD, MBA

From the Departments of Radiology (J.G., R.S., C.S., L.F., C.W.A.P.) and Orthopedic Surgery (S.R.), Balgrist University Hospital, University of Zurich, Forchstrasse 340, 8008 Zurich, Switzerland; and Department of Radiology, HFR, University of Fribourg, Fribourg, Switzerland (J.G.). Received August 26, 2019; revision requested October 15; revision received March 9, 2020; accepted March 17. Address correspondence to J.G.

Conflicts of interest are listed at the end of this article.

See also the editorial by Zanetti in this issue.

Radiology 2020; 296:98–108 • <https://doi.org/10.1148/radiol.2020191901> • Content code: 

**Background:** MRI with metal artifact reduction has gained importance in assessment of pain with total hip arthroplasty (THA). However, its role in diagnosis of periprosthetic joint infection (PJI) has not been well defined.

**Purpose:** To evaluate findings of PJI after THA and to determine the diagnostic performance of 1.5-T MRI with metal artifact reduction.

**Materials and Methods:** Dedicated compressed sensing–based slice encoding for metal artifact correction 1.5-T MRI examinations (from January 2015 to April 2018) in patients with THA PJI (infection group) and noninfected THA (control group) were retrospectively evaluated by two musculoskeletal radiologists. Fisher exact test was used to compare the groups. Sensitivity, specificity, and accuracy were evaluated for each finding. Interobserver reliability was assessed with  $\kappa$  statistics.

**Results:** Forty patients (mean age, 69 years  $\pm$  11 [standard deviation]; 26 men) in the infection group and 100 patients (mean age, 67 years  $\pm$  11; 42 men) in the control group were evaluated. Periosteal reaction, capsule edema, and intramuscular edema differed between the two groups ( $P < .001$  for each finding). Periosteal reaction was found in 31 of 40 patients with infection and 10 of 100 participants in the control group (sensitivity, 78%; specificity, 90%; accuracy, 86%); capsule edema was found in 33 of 40 (infection group) and five of 100 (control group) (sensitivity, 83%; specificity, 95%; accuracy, 91%); and intramuscular edema was found in 38 of 40 (infection group) and 14 of 100 (control group) (sensitivity, 95%; specificity, 86%; accuracy, 89%). Interobserver agreement was almost perfect, with  $\kappa$  values between 0.88 and 0.92. No difference between the two groups was found regarding the presence of osteolysis (infection group, 23 of 40; control group, 60 of 100), bone marrow edema (39 of 40 vs 87 of 100), effusion (20 of 40 vs 26 of 100), abductor tendon lesion (22 of 40 vs 62 of 100), or bursitis (14 of 40 vs 34 of 100) ( $P > .05$  for each finding).

**Conclusion:** The presence of periosteal reaction, capsule edema, and intramuscular edema after total hip arthroplasty at 1.5-T MRI with metal artifact reduction had a high accuracy in evaluation of periprosthetic joint infection.

© RSNA, 2020

Online supplemental material is available for this article.

Total hip arthroplasty (THA) is one of the most common orthopedic surgical procedures. Its frequency is expected to increase further, given our aging population with higher expectations about their physical activity and quality of life (1–3). The overall outcome of THA is excellent (4), but complications can occur. Among these, periprosthetic joint infection (PJI) is devastating. The rate of PJI after primary THA varies in the literature (5–7). It has been reported to be as high as 2.2% of patients after 10 years in a large epidemiologic study (5) and to contribute to about 15% of revision surgeries (8,9). Early detection of infection is crucial for successful treatment (10,11), but making the appropriate diagnosis can be challenging.

The diagnosis of PJI is based on a combination of clinical findings, laboratory evaluation of blood and synovial fluid, and intraoperative findings (10,12,13). Imaging is relevant for evaluation of differential diagnoses of PJI but is not part of the 2018 PJI diagnostic

criteria of the Musculoskeletal Infection Society (12). Conventional radiography is the first-line imaging tool for evaluation of THA. It gives information about the implant and adjacent bony structures. Rapid osteolysis suggests infection, but radiographs are of little value in soft-tissue assessment (14,15). US is helpful for assessing periprosthetic collections (16), but collections are not always present with PJI. CT has been proven more accurate for periprosthetic soft-tissue evaluation, such as assessment of joint or bursa distention, or fluid collections (17). However, alterations such as muscle edema or bone marrow edema can be difficult to identify with CT. Nuclear medicine examinations such as leukocyte–bone marrow scintigraphy or fluorodeoxyglucose PET have been shown to be sensitive for diagnosis of PJI but less accurate in identification of differential diagnoses (18).

Since the development of advanced metal artifact–reducing techniques, MRI has become an important

## Abbreviations

CS = compressed sensing, PJI = periprosthetic joint infection, SEMAC = slice encoding for metal artifact correction, STIR = short inversion time inversion recovery, THA = total hip arthroplasty

## Summary

MRI with metal artifact reduction at 1.5 T was sensitive and specific for the diagnosis of periprosthetic hip joint infection.

## Key Results

- The sensitivity and specificity of periosteal reaction for periprosthetic hip joint infection were 78% and 90%, respectively.
- The sensitivity and specificity of capsule edema for periprosthetic hip joint infection were 83% and 95%, respectively.
- The sensitivity and specificity of intramuscular edema for periprosthetic hip joint infection were 95% and 86%, respectively.

modality in the assessment of arthroplasties (19,20). MRI findings of PJI have been proposed (21); however, their specificity and sensitivity have not been evaluated. To the best of our knowledge, the only specific PJI MRI finding is lamellated synovitis in knee arthroplasty (22). The purpose of this study was to evaluate findings of periprosthetic infection after THA and to determine the diagnostic performance of 1.5-T MRI with metal artifact reduction.

## Materials and Methods

General written informed consent and permission to use the participants' data for research purposes were obtained at the time of the MRI examination. For this retrospective study, a waiver was given by the ethics committee that no additional specific informed consent was necessary.

## Study Sample

Patients with THA who were referred for hip MRI at Balgrist University Hospital from January 2015 to April 2018 were included in the study. All patients were older than 18 years.

**Infection group.**—Our clinical database was searched for patient files with the keywords *hip/infection* or *hip/loosening*. Patients with THA infection who had undergone MRI were included according to the following criteria: THA was performed more than 6 weeks before MRI; the patient met Musculoskeletal Infection Society criteria for the presence of a PJI (12) (Table E1 [online]); and the patient had a positive microbiologic finding from joint aspiration, an intraoperative sample, or both (obtained during revision surgery) based on use of standard methods for detection and identification of microorganisms, as previously described (23). The exclusion criterion was symptomatic THA after recent trauma.

**Control group.**—Our picture archiving and communication system was searched for metal artifact–reducing hip MRI examinations performed during the same period. Inclusion criteria were (a) MRI performed 6 weeks or more after THA and (b) 1 year of follow-up after MRI examination without any

sign of infection (no clinical or laboratory findings suggestive of infection). The exclusion criterion was the same as for the group with infections.

## MRI Examination

All patients underwent a standardized imaging protocol optimized for metal artifact reduction for hip prosthesis. MRI scans were acquired at 1.5 T (Magnetom Avanto Fit; Siemens Healthcare, Erlangen, Germany) by using an 18-channel surface coil and a 32-channel spine coil. The protocol included a compressed sensing (CS)–based coronal short inversion time inversion-recovery (STIR) slice encoding for metal artifact correction (SEMAC) sequence; an axial STIR sequence; and high-bandwidth sequences in standard planes (axial and sagittal T1, coronal T2). The CS SEMAC sequence was applied with 13 or 19 slice-encoding steps, 10 iterations, and a normalization factor of 0.001 to achieve optimal image quality (24). Detailed imaging parameters are listed in Table 1.

## MRI Analysis

All MRI examinations were anonymized and randomized by a person not involved in the analysis. The images were evaluated independently by two fellowship-trained musculoskeletal radiologists (J.G., C.S.; both with 7 years of experience in musculoskeletal MRI) who were blinded to clinical data and the final diagnosis of hip infection. The readout was spread over 3 months for both readers (two to three examinations per day).

**Periprosthetic bone.**—Periprosthetic bone was assessed for the femur in each of the Gruen zones (25) and for the acetabulum in the DeLee and Charnley zones (26). For clarity, periprosthetic bone regions were summarized as acetabulum (DeLee and Charnley zones I, II, and III), entire shaft (Gruen zones 1–14), proximal shaft (Gruen zones 1, 7, 8, and 14), middle shaft (Gruen zones 2, 6, 9, and 13), and distal shaft (Gruen zones 3, 4, 5, 10, 11, and 12).

The following findings were evaluated: presence of peri-implant lysis (defined as bone loss of 2 mm or more at bone-implant interface), bone marrow edema (defined as intramedullary hyperintensity on STIR sequence images), and periosteal reaction (defined as periosteal linear hyperintensity on STIR sequence images).

**Joint.**—The prosthetic hip joint was evaluated for effusion (<3 mm, 3–6 mm, >6 to 10 mm, >10 to 20 mm, and >20 mm), measured as radial width between the prosthetic neck and joint capsule. Findings were categorized according to measurement (positive when greater than 10 mm), capsule appearance (hypointense, edematous, lamellated), and medial and lateral capsule thickness (<3 mm, 3–6 mm, >6 mm; summarized as positive when >6 mm).

**Periprosthetic soft tissues.**—Periprosthetic soft tissues (muscles, subcutaneous tissues) were assessed for the presence of edema, fluid collection, or both, and its distribution (subcutaneous, intramuscular, along the surgical approaches). The

**Table 1: 1.5-T Hip MRI Protocol Optimized for Metal Artifact Reduction**

Parameter	Coronal STIR CS- SEMAC Sequence	Axial STIR WARP*	Coronal T2 High- Bandwidth Sequence	Axial T1 High- Bandwidth Sequence	Sagittal T1 High- Bandwidth Sequence
TR/TE (msec)	4220/36	4000/31	4000/58	669/8.6	627/7.3
Refocusing flip angle (degrees)	140	150	150	180	180
Echo train length	9	11	15	3	3
No. of signals acquired	1	3	2	2	2
No. of slices	25	27	20	29	31
Section thickness (mm)	4	7	4	6	4
Spacing (mm)	4	8.75	6	8.4	4.4
Matrix	256 × 205	384 × 269	512 × 282	512 × 410	320 × 320
Field of view (mm <sup>2</sup> )	280 × 280	189 × 189	220 × 220	210 × 210	200 × 200
Bandwidth (Hz/pixel)	500	450	390	425	435
Inversion time (msec)	160	150	...	...	...
Slice encoding steps	19/13	...	...	...	...
Acquisition time (min:sec)	06:19/05:01	03:56	02:28	02:17	01:59

Note.—CS = compressed sensing, SEMAC = slice encoding for metal artifact correction, STIR = short inversion time inversion recovery, TE = echo time, TR = repetition time.

\* WARP; Siemens Healthcare, Munich, Germany.

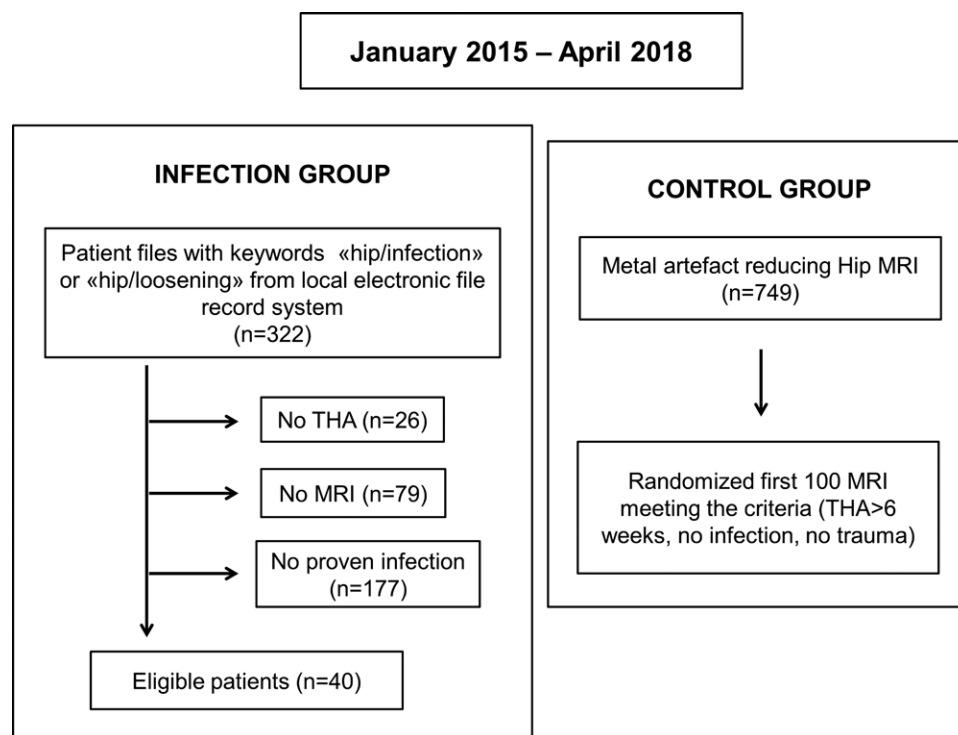


**Figure 1:** Flowchart shows patient inclusion and exclusion criteria. THA = total hip arthroplasty.

features of a fluid collection, namely septations, communication with articulation, or both, were evaluated. Abductor tendons (gluteus medius and minimus) were classified regarding tendon quality (normal, tendinopathy, partial tear, avulsion), and the result was considered positive in the case of a partial tear or avulsion. The presence of bursitis (trochanteric, iliopsoas, or both) and inguinal adenopathy was also evaluated.

### Statistical Analysis

Statistical analysis was performed with software (SPSS, version 23; IBM, Armonk, NY). The  $\kappa$  statistic was used to assess interobserver agreement; a  $\kappa$  value less than 0 was defined as no agreement, a  $\kappa$  value of 0–0.20 was defined as slight agreement, a  $\kappa$  value of 0.21–0.40 was defined as fair agreement, a  $\kappa$  value of 0.41–0.60 was defined as moderate agreement, a  $\kappa$  value of 0.61–0.80 was defined as substantial

**Table 2: Patient Characteristics for Infection and Control Groups**

Characteristic	Infection Group ( <i>n</i> = 40)	Control Group ( <i>n</i> = 100)	<i>P</i> Value
<b>Patients</b>			
Age (y)*	69 ± 11	67 ± 11	.59
Sex	...	...	.02
Male	26	42	...
Female	14	58	...
Body mass index (kg/m <sup>2</sup> )†	29 (18–40)	28 (18–43)	.09
Diabetes	6	7	.13
<b>THA</b>			
Side	...	...	.26
Right	25	49	...
Left	15	51	...
Type of arthroplasty	...	...	.06
Metal or ceramic/polyethylene	38	82	...
Metal/metal	2	18	...
Cemented	7	12	.41
<b>Indication for THA</b>			
Primary OA	31	76	...
Secondary OA	4	13	...
Dysplasia	0	8	...
Osteonecrosis	2	1	...
Perthes	0	2	...
Posttraumatic	2	2	...
Fracture	5	11	...
Revised THA	14	24	.52
Infection	4	4	...
Abductor insufficiency	0	4	...
Implant related	7	12	...
Luxation	2	4	...
Periprosthetic fracture	1	0	...
<b>MRI</b>			
Mean interval between arthroplasty and MRI (mo)†	46 (2–264)	100 (7–371)	.001
<b>MRI indication</b>			
Suspicion of infection	22	7	...
Suspicion of loosening	6	26	...
Abductor evaluation	7	41	...
Suspicion of implant-related complications	0	17	...
Nonspecific pain	5	9	...

Note.—OA = osteoarthritis, THA = total hip arthroplasty.

\* Data are mean ± standard deviation.

† Data are the mean, and data in parentheses are the range.

agreement, and a  $\kappa$  value of 0.81–1 was defined as almost perfect agreement (27,28). The  $\chi^2$  test and Fisher exact test were used to determine whether there was a difference between the frequencies of the findings between groups. As 12 findings were evaluated, *P* values were adjusted by using Bonferroni correction; *P* < .004 indicates a significant difference. Sensitivity, specificity, and accuracy were evaluated for each finding. Exact McNemar test was used to compare sensitivity, specificity, and accuracy between the two readers. For demographic data, the *t*,  $\chi^2$ , and Fisher exact tests were applied to compare the groups.

## Results

### Patient Characteristics

We identified 322 patient files with the keywords *hip/infection* or *hip/loosening*. Twenty-six patients had not undergone THA, and 79 patients had never undergone hip MRI. Of the remaining patients, 177 did not meet the criteria for PJI (Fig 1). The infection group consisted of 40 patients with THA infection (14 women, 26 men; mean age, 69 years ± 11 [standard deviation]). Twenty-six patients had undergone

**Table 3: Frequency, Statistical Significance, and  $\kappa$  Values**

Finding and Location	Reader 1			Reader 2			κ Value
	Infection Group ( <i>n</i> = 40)	Control Group ( <i>n</i> = 100)	<i>P</i> Value	Infection Group ( <i>n</i> = 40)	Control Group ( <i>n</i> = 100)	<i>P</i> Value	
Osteolysis >2 mm							
Shaft							
Entire	23	60	.85	26	70	.69	0.76 (0.61, 0.87)
Proximal third	23	59	>.99	25	66	.7	0.76 (0.63, 0.87)
Middle third	13	33	>.99	16	44	.71	0.61 (0.48, 0.74)
Distal third	6	12	.59	7	14	.1	0.66 (0.49, 0.79)
Acetabulum	9	25	.83	13	34	>.99	0.7 (0.57, 0.82)
Bone edema							
Shaft							
Entire	39	87	.06	38	95	>.99	0.33 (0.04, 0.60)
Proximal third	36	82	.03	35	87	>.99	0.48 (0.24, 0.67)
Middle third	29	73	>.99	35	85	.8	0.41 (0.23, 0.57)
Distal third	32	46	<.001*	33	65	.04	0.52 (0.39, 0.66)
Acetabulum	24	59	>.99	28	60	.33	0.42 (0.25, 0.57)
Periosteal reaction							
Shaft							
Entire	31	10	<.001*	32	14	<.001*	0.92 (0.84, 0.98)
Proximal third	24	2	<.001*	28	2	<.001*	0.87 (0.75, 0.96)
Middle third	28	5	<.001*	25	11	<.001*	0.79 (0.65, 0.90)
Distal third	19	6	<.001*	18	7	<.001*	0.95 (0.87, 1)
Acetabulum	19	4	<.001*	29	7	<.001*	0.72 (0.58, 0.86)
Effusion	20	26	.009	24	25	<.001*	0.63 (0.49, 0.76)
Capsule edema	33	5	<.001*	31	8	<.001*	0.88 (0.77, 0.95)
Capsule thickness >6 mm							
Lateral	23	18	<.001*	14	13	.004	0.42 (0.25, 0.59)
Medial	19	7	<.001*	8	6	.25	0.37 (0.15, 0.56)
Subcutaneous edema	31	22	<.001*	30	29	<.001*	0.85 (0.75, 0.93)
Intramuscular edema							
Overall	38	14	<.001*	39	15	<.001*	0.88 (0.78, 0.95)
Along surgical approach	31	9	<.001*	33	11	<.001*	0.73 (0.59, 0.85)
Nonsurgical approach	36	6	<.001*	37	7	<.001*	0.87 (0.76, 0.95)
Abductor tendon lesion							
Gluteus minimus	16	40	>.99	26	63	.85	0.8 (0.70, 0.91)
Gluteus medius	22	62	.45	16	41	>.99	0.78 (0.66, 0.88)
Fluid collection							
Subcutaneous							
Along surgical approach	14	5	<.001*	17	4	<.001*	0.7 (0.50, 0.87)
Nonsurgical approach	3	0	.02	1	0	.29	0.5 (0, 1)
Intramuscular (subfascial)							
Along surgical approach	23	7	<.001*	24	7	<.001*	0.77 (0.62, 0.88)
Nonsurgical approach	11	2	<.001*	9	1	<.001*	0.68 (0.42, 0.81)
Articular communication	23	8	<.001*	21	12	<.001*	0.76 (0.61, 0.88)
Septation	23	4	<.001*	19	7	<.001*	0.74 (0.59, 0.88)
Bursitis							
Trochanteric	14	34	>.99	14	35	>.99	0.8 (0.69, 0.89)
Iliopsoas	7	9	.32	10	10	.03	0.81 (0.63, 0.94)
Inguinal adenopathy	6	0	<.001*	9	0	<.001*	0.79 (0.43, 1)

Note.—Data represent different findings for both readers for both groups. Except where otherwise specified, data are numbers of patients; 95% confidence intervals are in parentheses.

\* Data indicate a significant difference.



**Table 4: Total Hip Arthroplasty Periprosthetic Joint Infection at MRI: Diagnostic Performance of Most Relevant Findings**

Finding and Location	Sensitivity (%)	Specificity (%)	Accuracy (%)
Periosteal reaction, shaft	78 (61.6, 89.2) [31/40]	90 (82.4, 95.1) [90/100]	86 (79.6, 91.6) [121/140]
Capsule edema	83 (67.2, 92.7) [33/40]	95 (88.7, 98.4) [95/100]	91 (85.5, 95.5) [128/140]
Intramuscular edema			
Overall	95 (83.1, 99.4) [38/40]	86 (77.6, 92.1) [86/100]	89 (82.1, 93.3) [124/140]
Along surgical approach	78 (61.6, 89.2) [31/40]	91 (83.6, 95.8) [91/100]	87 (80.4, 92.2) [122/140]
Nonsurgical approach	90 (76.3, 97.2) [36/40]	94 (87.4, 97.8) [94/100]	93 (87.3, 96.5) [130/140]
Fluid collection			
Intramuscular (subfascial), surgical approach	58 (40.9, 73.0) [23/40]	93 (86.1, 97.1) [93/100]	83 (75.6, 88.7) [116/140]
Intramuscular (subfascial), nonsurgical approach	28 (14.6, 43.9) [11/40]	98 (93.0, 99.8) [98/100]	78 (70.0, 84.4) [109/140]
Articular communication	58 (40.9, 73.0) [23/40]	92 (84.8, 96.5) [92/100]	82 (74.8, 88.1) [115/140]
Septation	58 (40.9, 73.0) [23/40]	96 (90.1, 98.9) [96/100]	85 (78.0, 90.5) [119/140]

Note.—Data shown are for reader 1. Data in parentheses are 95% confidence intervals, and raw data are in brackets.

a primary THA, and 14 (35%) of 40 patients had undergone a revision. The mean interval between arthroplasty and MRI was 46 months (range, 6 weeks to 264 months). Twenty-seven patients had positive microbiologic findings with joint aspiration and surgery sampling, nine had positive findings with surgery sampling only, and four had positive findings with joint aspiration only. The pathogens found with culture were the following: *Staphylococcus epidermidis* (11 cases), *Staphylococcus aureus* (seven cases), *Propionibacterium avidum* (five cases), *Propionibacterium acnes* (three cases), methicillin-resistant *Staphylococcus aureus* (two cases), *Streptococcus dysgalactiae* (two cases), other *Streptococcus* species (*pneumoniae* and *agalactiae*, one case each), other *Staphylococcus* species (*caprae* and *saccharolyticus*, one case each), *Anaerococcus murdochii* (one case), *Enterococcus faecium* (one case), *Escherichia coli* (one case), *Klebsiella pneumoniae* (one case), *Morganella morganii* (one case), and mixed flora infection (*Finnegoldia magna*, *Proteus mirabilis*, and *Actinomyces europaeus*; one case).

The control group consisted of 100 patients (58 women, 42 men; mean age, 67 years  $\pm$  11 [standard deviation]). Seventy-six patients had undergone primary THA, and 24 (24%) had undergone revision. The mean interval between arthroplasty and MRI was 100 months (range, 7–371 months). Thirty-five patients had undergone joint aspiration (indications: before every revision surgery, exclusion of low-grade infection) with no sign of infection. The diagnoses were as follows: 52 musculotendinous complications (abductor tendon tear, iliopsoas irritation or impingement, iliotibial band disorder); 25 cases of aseptic loosening; 13 other implant-related complications (wear, dislocation, metallosis, pseudotumor); eight cases of trochanteric bursitis; one stress fracture; and one case of symptomatic heterotopic ossifications.

Detailed demographic data for both groups are shown in Table 2.

### MRI Findings

MRI findings and their diagnostic performance in the detection of PJI are detailed in Tables 3, 4, and E2 (online). The difference between the PJI and control groups was significant ( $P < .004$ ) for both readers for the following findings: periosteal reaction, capsular edema, subcutaneous edema, intramuscular edema, subcutaneous fluid collection in the area of surgical approach, intramuscular fluid collection, presence of articular communication or septation of collections, and inguinal adenopathy.

The presence of periosteal reaction (Fig 2), capsule edema (Fig 3), or intramuscular edema (Fig 4) was most significant for diagnosing PJI. For reader 1, shaft periosteal reaction demonstrated a sensitivity of 78%, a specificity of 90%, and an accuracy of 86% in the detection of PJI. Capsule edema showed a sensitivity of 83%, a specificity of 95%, and an accuracy of 91%. For intramuscular edema, the values were 95%, 86%, and 89%, respectively. The intramuscular location of a fluid collection, its communication with the joint, and the presence of septation were highly specific (93%, 92%, and 96%, respectively), although less sensitive (58% for each finding) (Fig 5). Sensitivity, specificity, and accuracy of the aforementioned findings from reader 2 were not statistically different from those of reader 1 (all  $P > .6$ ).

No difference between the groups was found regarding the presence of shaft osteolysis (reader 1,  $P = .85$ ; reader 2,  $P = .69$ ), acetabulum osteolysis (reader 1,  $P = .83$ ; reader 2,  $P > .99$ ), shaft bone marrow edema (reader 1,  $P = .06$ ; reader 2,  $P > .99$ ), acetabulum bone marrow edema (reader 1,  $P > .99$ ; reader 2,  $P = .33$ ), effusion (reader 1,  $P = .009$ ; reader 2,  $P < .001$ ), gluteus minimus lesion (reader 1,  $P > .99$ ; reader 2,  $P =$



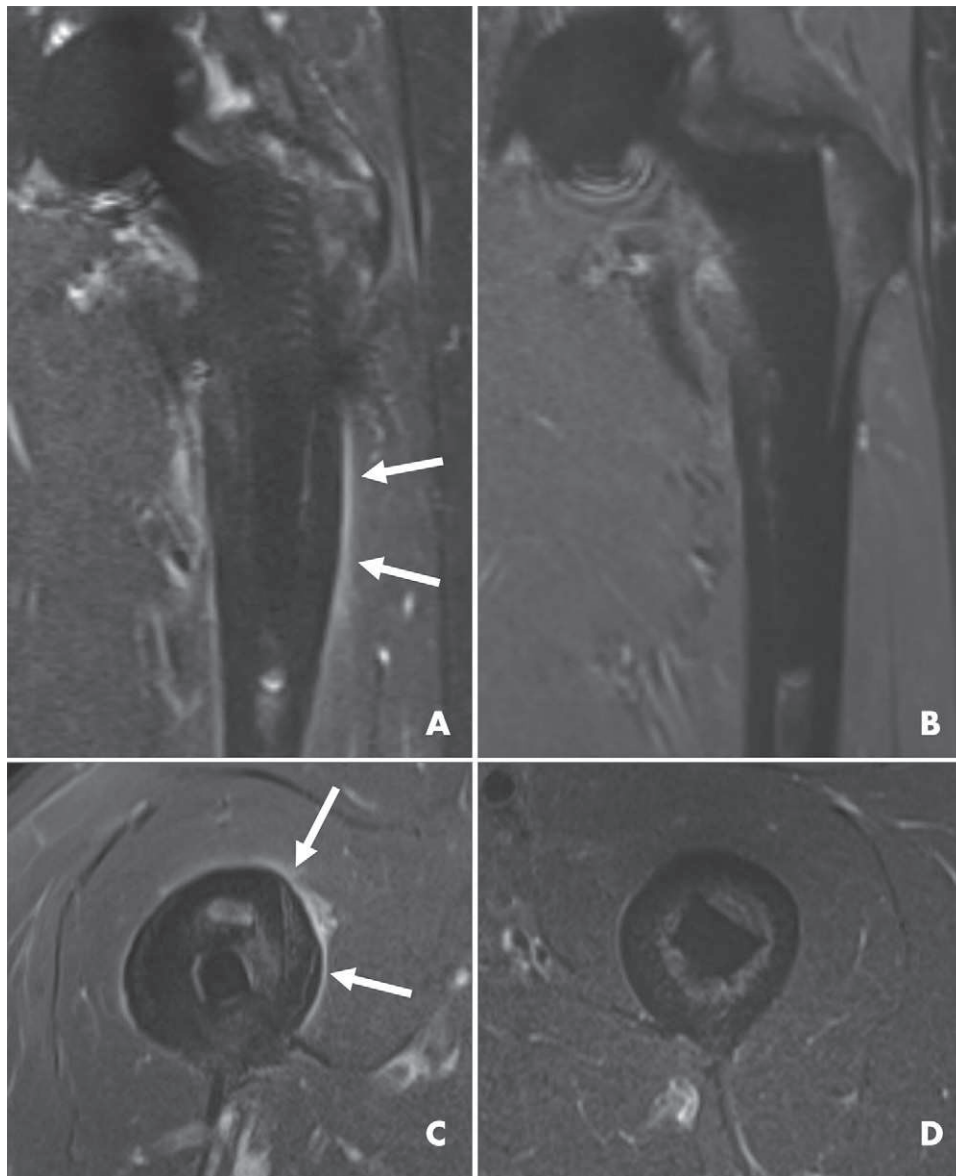


**Figure 2:** MRI scans show periosteal reaction. A, B, Coronal short inversion time inversion-recovery (STIR) compressed sensing slice encoding for metal artifact correction and, C, D, axial STIR MR images in four patients. In, A, and, C, linear hyperintensity (arrows) represents periosteal reaction in two patients with proven total hip arthroplasty periprosthetic joint infection. B, D, For comparison, images in patients from the control group without periosteal reaction are shown.

.85), gluteus medius lesion (reader 1,  $P = .45$ ;  $P > .99$ ), medial (reader 1,  $P < .001$ ; reader 2,  $P = .25$ ) and lateral (reader 1,  $P < .001$ ; reader 2,  $P = .004$ ) capsule thickness, trochanteric bursitis (reader 1,  $P > .99$ ; reader 2,  $P > .99$ ), or iliopsoas bursitis (reader 1,  $P = .32$ ; reader 2,  $P = .03$ ). There was no lamellated morphologic appearance of the joint capsule found by either reader in any of the cases.

#### Interobserver Agreement

Interobserver agreement was almost perfect for periosteal reaction ( $\kappa = 0.92$ ), capsule edema ( $\kappa = 0.88$ ), muscle edema ( $\kappa = 0.88$ ), and subcutaneous edema ( $\kappa = 0.85$ ); substantial for bursitis ( $\kappa = 0.80$ ), adenopathy ( $\kappa = 0.79$ ), intramuscular collection ( $\kappa = 0.77$ ), communication of collection with joint

( $\kappa = 0.76$ ), presence of collection septation ( $\kappa = 0.74$ ), and subcutaneous collection ( $\kappa = 0.71$ ); and moderate for bone marrow edema ( $\kappa = 0.48$ ) and capsule thickness ( $\kappa = 0.43$ ).

#### Discussion

Periprosthetic joint infection (PJI) after total hip arthroplasty (THA) is a serious complication and must be diagnosed as soon as possible because early management is critical to minimize morbidity. MRI has been shown to be effective in evaluation of painful hip arthroplasty (21,29); however, to our knowledge, no specific MRI findings for PJI have been described. This study examined the value of MRI in assessing PJI after THA. The presence of periosteal reaction, capsule edema, or intramuscular edema was

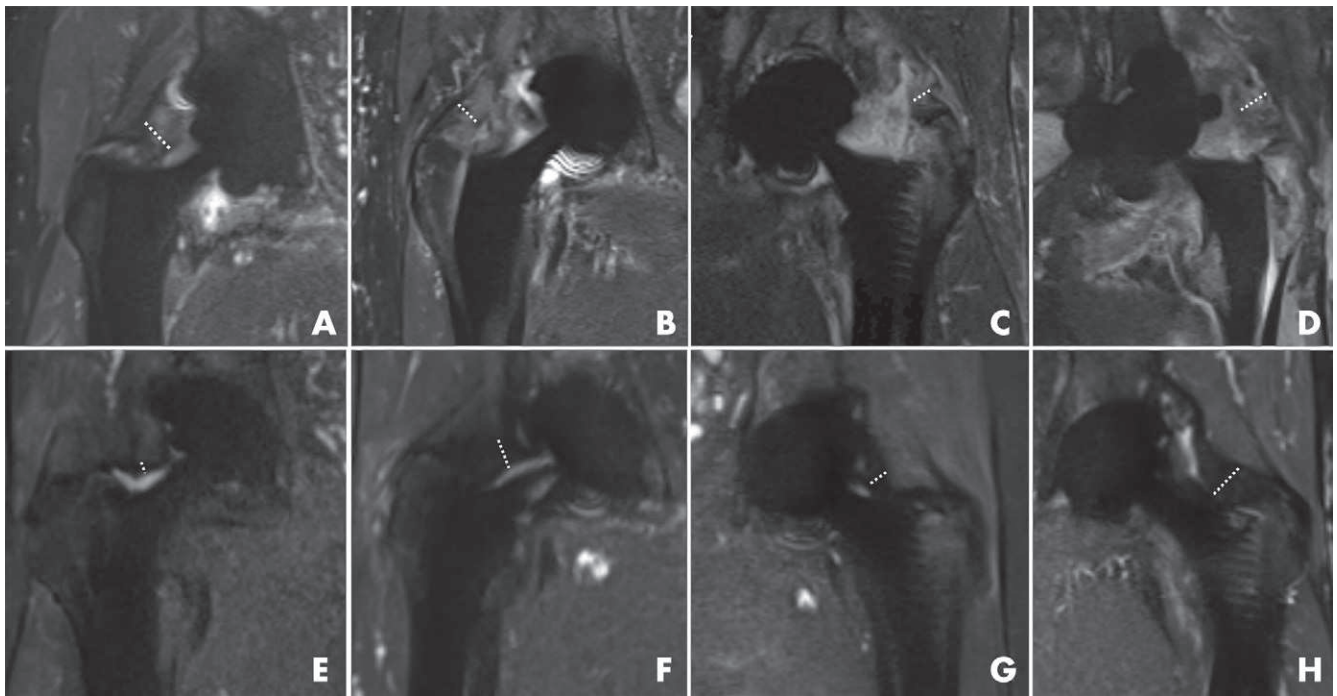


**Figure 3:** Coronal short inversion time inversion-recovery compressed sensing slice encoding for metal artifact correction MRI scans show capsule edema in eight different patients with total hip arthroplasty (THA). A–D, Images in four patients with periprosthetic joint infection. MRI scans demonstrate thickened capsule (dotted lines) with capsule hyperintensity corresponding to capsule edema. E–H, Images in four patients without THA infection depict variable capsular thickness (dotted lines) but no capsule edema.

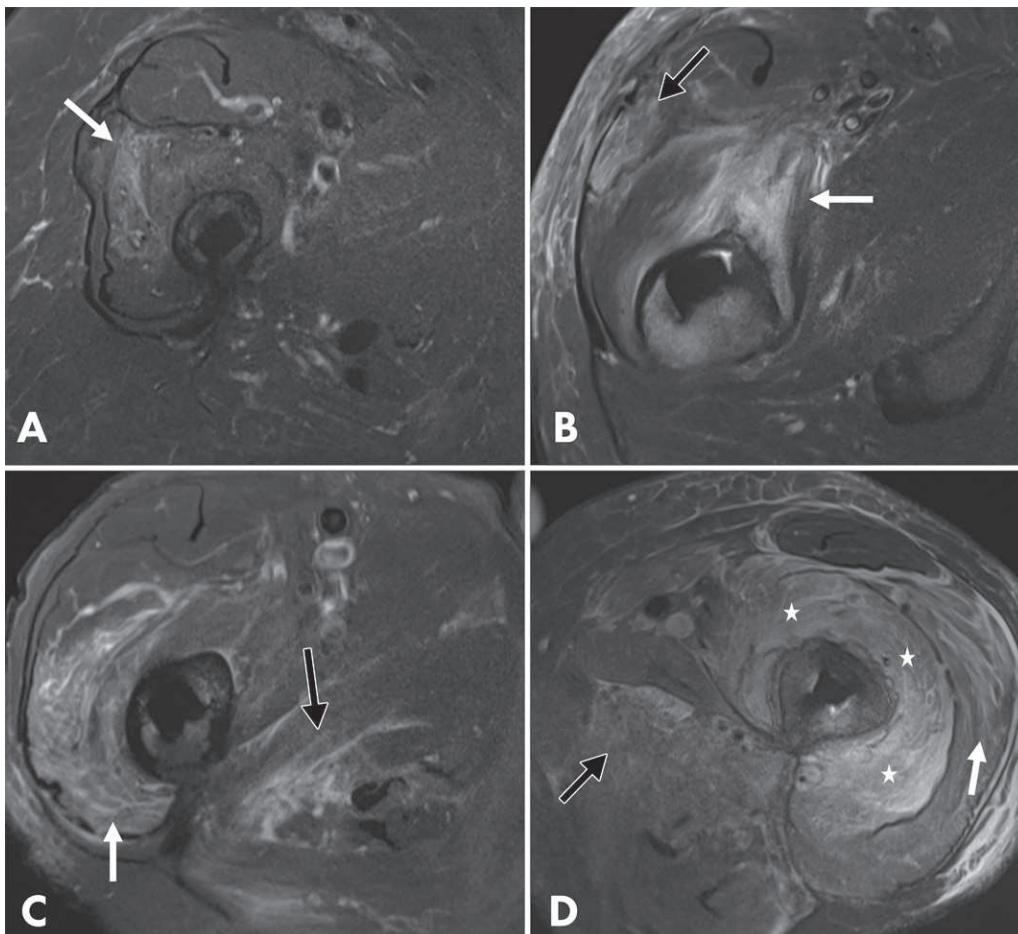


**Figure 4:** Axial short inversion time inversion recovery MRI scans show intramuscular edema in four different patients with proven periprosthetic joint infection with different amounts of edema: A, mild; B, C, moderate; and D, severe. A, Intramuscular hyperintensity (arrow) corresponds to mild intramuscular edema in the vastus intermedius. B, Image shows moderate edema in the vastus medialis (white arrow) and tensor fasciae latae (black arrow). C, Image shows moderate edema in the vastus lateralis (white arrow) and adductor magnus (black arrow). D, Image shows severe edema in the vastus lateralis (white arrow), adductor magnus (black arrow), and vastus intermedius (★).

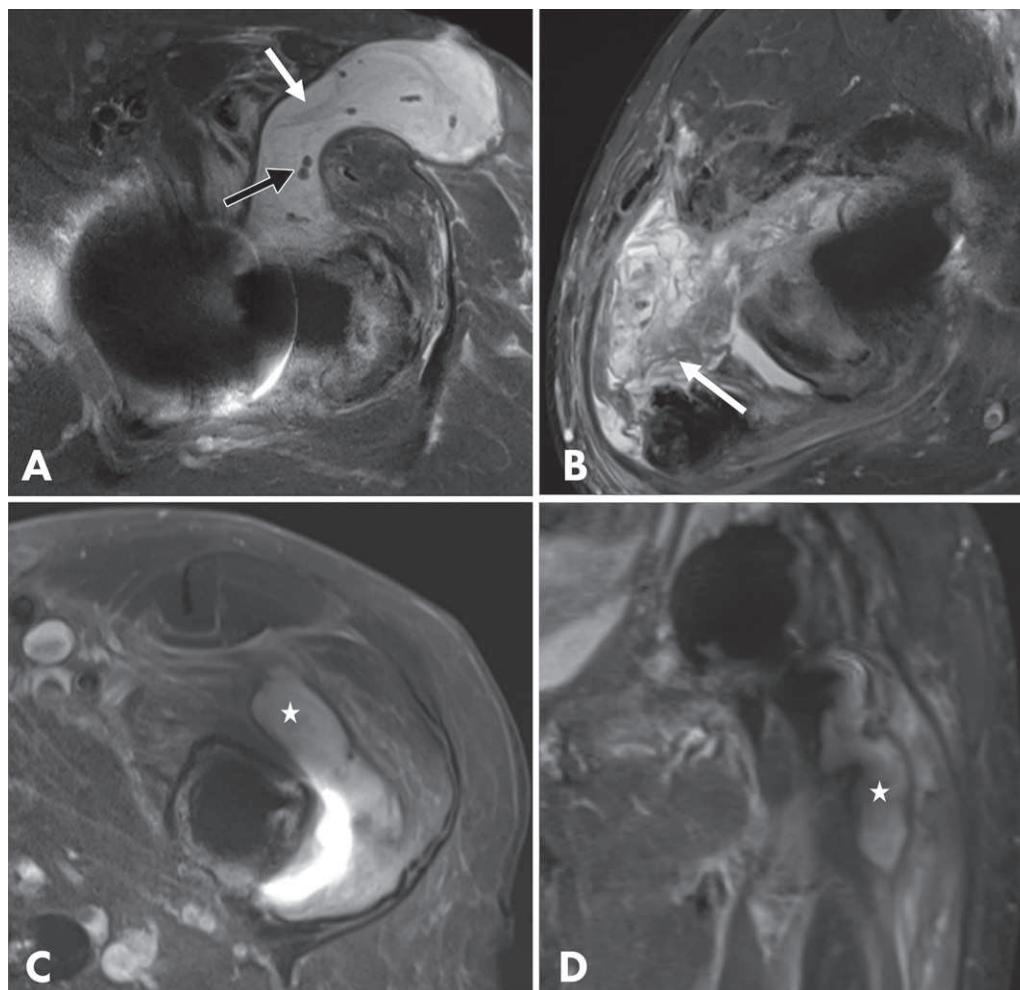


**Figure 5:** MRI scans show collections in different patients with proven periprosthetic joint infection. A, Axial short inversion time inversion-recovery (STIR) MRI scan shows subcutaneous collection with articular communication. Note thin septations (white arrow) and debris (black arrow). B, Axial STIR MRI scan shows thick septations (arrow) in subfascial collection. C, Axial STIR and, D, coronal STIR compressed sensing slice encoding for metal artifact correction images in the same patient depict intramuscular collection (in the vastus intermedius) (★).

significantly different between the groups ( $P < .004$ ) and showed high sensitivity (78%, 83%, and 95%, respectively), specificity (90%, 95%, and 86%, respectively), and accuracy (86%, 91%, and 89%, respectively) for PJI.

Patients with PJI can present with acute symptoms, including pain, swollen joints, fever, or the presence of a sinus tract (30). Nevertheless, the clinical presentation can be nonspecific. The criteria proposed by the Musculoskeletal Infection Society (12) are based on synovial, serum, and intraoperative findings. Because joint aspiration has better diagnostic accuracy than serum analysis (31), it is usually essential for the diagnosis of PJI. In addition to microbiologic culture, different synovial markers have been introduced: leukocyte count, polymorphonucleocyte percentage, levels of C-reactive protein,  $\alpha$ -defensin, leukocyte-esterase, and interleukins. According to a meta-analysis (32), all of these show a high specificity (range, 86%–96%) and an overall sensitivity greater than 80%, except for culture, which has a lower sensitivity of only 62%. Indications for diagnostic

joint aspiration remain broad because of the often nonspecific clinical symptoms (33,34). Thus, additional diagnostic criteria, such as imaging findings, would be valuable to better select and reduce the number of patients undergoing joint aspiration.

In the American College of Radiology Appropriateness Criteria for evaluation of painful THA, radiography is considered to be the first examination (35). New and fast-developing periprosthetic osteolysis is suggestive of infection, but radiographic findings are often normal (15,17,36). US is useful in evaluating soft tissues and is almost comparable to MRI in detecting periprosthetic collections (16). Its value in assessing muscle edema and vascularization (37,38) has never been evaluated in the context of PJI, and evaluation of deep alterations can be challenging. CT, however, was shown by Cyteval et al (17) to be sensitive and specific when at least one soft-tissue abnormality (joint distention, fluid-filled bursae, or fluid collections) was used to diagnose PJI. They found a sensitivity of 41% and a specificity of 100% for intra- or



perimuscular fluid collections. Our results are consistent with these findings for intramuscular fluid collection (sensitivity range, 28%–58%; specificity range, 75%–100%). Although intramuscular collections are specific for PJI, they are not always present. Periosteal bone formation was found by Cyteval et al (17) to be very specific (100%) but with low sensitivity (16%). In our study, periosteal reaction was highly specific (90%) and sensitive (78%).

In native joints, MRI is the imaging modality of choice when septic arthritis is suspected. Synovial enhancement or thickening, perisynovial edema, periarticular soft-tissue edema, periosteal reaction, and concomitant osteomyelitis are associated with septic arthritis (39,40). Our findings for PJI in the setting of THA are similar with regard to capsule edema, muscle edema, and collections.

Leukocyte scintigraphy and PET have been shown to be highly accurate in diagnosis of PJI, with sensitivity ranging from 69% to 88% and specificity ranging from 75% to 96% (18,41–43). Our results show that MRI has diagnostic accuracy within this range, with sensitivity between 78% and 95% and specificity ranging from 86% to 95%. However, these nuclear examinations are often nonspecific regarding potential differential diagnoses.

A limitation of our study was that only a subset of the control group underwent joint aspiration; some patients were not initially referred because PJI was suspected or did not fulfill the criteria for aspiration. Although the control group did not show signs of infection at follow-up, the possibility of a low-grade infection cannot be completely excluded. Another limitation was that the control group consisted only of symptomatic patients. An evaluation of findings in asymptomatic populations would be helpful for comparison. Finally, no multivariable analysis was performed.

In conclusion, the presence of periosteal reaction, capsule edema, and intramuscular edema after total hip arthroplasty at 1.5-T MRI with metal artifact reduction had a high accuracy in evaluation of periprosthetic joint infection. Imaging is currently not part of the Musculoskeletal Infection Society criteria for diagnosing periprosthetic joint infection; however, with advances in MRI, this recommendation may be changed in the future.

**Author contributions:** Guarantor of integrity of entire study, J.G.; study concepts/study design or data acquisition or data analysis/interpretation, all authors; manuscript drafting or manuscript revision for important intellectual content, all authors; approval of final version of submitted manuscript, all authors; agrees to ensure any questions related to the work are appropriately resolved, all authors; literature research, J.G., L.F., S.R., C.W.A.P.; clinical studies, J.G., C.S., L.F., C.W.A.P.; statistical analysis, J.G.; and manuscript editing, J.G., C.S., L.F., S.R., C.W.A.P.

**Disclosures of Conflicts of Interest:** J.G. disclosed no relevant relationships. R.S. disclosed no relevant relationships. C.S. disclosed no relevant relationships. L.F. disclosed no relevant relationships. S.R. disclosed no relevant relationships. C.W.A.P. disclosed no relevant relationships.

## References

- Singh JA. Epidemiology of knee and hip arthroplasty: a systematic review. *Open Orthop J* 2011;5(1):80–85.
- Maradit Kremers H, Larson DR, Crowson CS, et al. Prevalence of Total Hip and Knee Replacement in the United States. *J Bone Joint Surg Am* 2015;97(17):1386–1397.
- Courpied JP, Caton JH. Total Hip Arthroplasty, state of the art for the 21st century. *Int Orthop* 2011;35(2):149–150.
- Shan L, Shan B, Graham D, Saxena A. Total hip replacement: a systematic review and meta-analysis on mid-term quality of life. *Osteoarthritis Cartilage* 2014;22(3):389–406.
- Ong KL, Kurtz SM, Lau E, Bozic KJ, Berry DJ, Parvizi J. Prosthetic joint infection risk after total hip arthroplasty in the Medicare population. *J Arthroplasty* 2009;24(6 Suppl):105–109.
- Phillips JE, Crane TP, Noy M, Elliott TSJ, Grimer RJ. The incidence of deep prosthetic infections in a specialist orthopaedic hospital: a 15-year prospective survey. *J Bone Joint Surg Br* 2006;88(7):943–948.
- Triantafyllopoulos GK, Soranoglou VG, Memtsoudis SG, Sculco TP, Poulosides LA. Rate and Risk Factors for Periprosthetic Joint Infection Among 36,494 Primary Total Hip Arthroplasties. *J Arthroplasty* 2018;33(4):1166–1170.
- Bozic KJ, Kurtz SM, Lau E, Ong K, Vail TP, Berry DJ. The epidemiology of revision total hip arthroplasty in the United States. *J Bone Joint Surg Am* 2009;91(1):128–133.
- Gwam CU, Mistry JB, Mohamed NS, et al. Current Epidemiology of Revision Total Hip Arthroplasty in the United States: National Inpatient Sample 2009 to 2013. *J Arthroplasty* 2017;32(7):2088–2092.
- Matthews PC, Berendt AR, McNally MA, Byren I. Diagnosis and management of prosthetic joint infection. *BMJ* 2009;338:b1773.
- Osmon DR, Berbari EF, Berendt AR, et al. Diagnosis and management of prosthetic joint infection: clinical practice guidelines by the Infectious Diseases Society of America. *Clin Infect Dis* 2013;56(1):e1–e25.
- Parvizi J, Tan TL, Goswami K, et al. The 2018 Definition of Periprosthetic Hip and Knee Infection: An Evidence-Based and Validated Criteria. *J Arthroplasty* 2018;33(5):1309–1314.e2.
- Beam E, Osmon D. Prosthetic Joint Infection Update. *Infect Dis Clin North Am* 2018;32(4):843–859.
- Cyteval C, Bourdon A. Imaging orthopedic implant infections. *Diagn Interv Imaging* 2012;93(6):547–557.
- Stumpe KDM, Nötzli HP, Zanetti M, et al. FDG PET for differentiation of infection and aseptic loosening in total hip replacements: comparison with conventional radiography and three-phase bone scintigraphy. *Radiology* 2004;231(2):333–341.
- Sdao S, Orlandi D, Aliprandi A, et al. The role of ultrasonography in the assessment of peri-prosthetic hip complications. *J Ultrasound* 2014;18(3):245–250.
- Cyteval C, Hamm V, Sarrahere MP, Lopez FM, Maury P, Taourel P. Painful infection at the site of hip prosthesis: CT imaging. *Radiology* 2002;224(2):477–483.
- Verberne SJ, Raijmakers PG, Temmerman OPP. The Accuracy of Imaging Techniques in the Assessment of Periprosthetic Hip Infection: A Systematic Review and Meta-Analysis. *J Bone Joint Surg Am* 2016;98(19):1638–1645.
- Hayter CL, Gold SL, Koff MF, et al. MRI findings in painful metal-on-metal hip arthroplasty. *AJR Am J Roentgenol* 2012;199(4):884–893.
- Talbot BS, Weinberg EP. MR Imaging with Metal-suppression Sequences for Evaluation of Total Joint Arthroplasty. *RadioGraphics* 2016;36(1):209–225.
- Fritz J, Lurie B, Miller TT, Potter HG. MR imaging of hip arthroplasty implants. *RadioGraphics* 2014;34(4):E106–E132.
- Plodkowski AJ, Hayter CL, Miller TT, Nguyen JT, Potter HG. Lamellated hyperintense synovitis: potential MR imaging sign of an infected knee arthroplasty. *Radiology* 2013;266(1):256–260.
- Bossard DA, Ledergerber B, Zingg PO, et al. Optimal Length of Cultivation Time for Isolation of *Propionibacterium acnes* in Suspected Bone and Joint Infections Is More than 7 Days. *J Clin Microbiol* 2016;54(12):3043–3049.
- Jungmann PM, Bensler S, Zingg P, Fritz B, Pfirrmann CW, Sutter R. Improved Visualization of Juxtaarticular Tissue Using Metal Artifact Reduction Magnetic Resonance Imaging: Experimental and Clinical Optimization of Compressed Sensing SEMAC. *Invest Radiol* 2019;54(1):23–31.
- Gruen TA, McNeice GM, Amstutz HC. “Modes of failure” of cemented stem-type femoral components: a radiographic analysis of loosening. *Clin Orthop Relat Res* 1979;(141):17–27.
- DeLee JG, Charnley J. Radiological demarcation of cemented sockets in total hip replacement. *Clin Orthop Relat Res* 1976;(121):20–32.
- Landis JR, Koch GG. The measurement of observer agreement for categorical data. *Biometrics* 1977;33(1):159–174.
- Kundel HL, Polansky M. Measurement of observer agreement. *Radiology* 2003;228(2):303–308.
- Agten CA, Sutter R, Dora C, Pfirrmann CWA. MR imaging of soft tissue alterations after total hip arthroplasty: comparison of classic surgical approaches. *Eur Radiol* 2017;27(3):1312–1321.
- Tande AJ, Patel R. Prosthetic joint infection. *Clin Microbiol Rev* 2014;27(2):302–345.
- Shahi A, Tan TL, Kheir MM, Tan DD, Parvizi J. Diagnosing Periprosthetic Joint Infection: And the Winner Is? *J Arthroplasty* 2017;32(9S):S232–S235.

32. Lee YS, Koo KH, Kim HJ, et al. Synovial Fluid Biomarkers for the Diagnosis of Periprosthetic Joint Infection. A Systematic Review and Meta-Analysis. *J Bone Joint Surg Am* 2017;99(24):2077–2084.
33. Berbari EF, Osmon DR, Lahr B, et al. The Mayo prosthetic joint infection risk score: implication for surgical site infection reporting and risk stratification. *Infect Control Hosp Epidemiol* 2012;33(8):774–781.
34. American Academy of Orthopaedic Surgeons. Diagnosis and Prevention of Periprosthetic Joint Infections Clinical Practice Guideline. <https://www.aaos.org/pjiguideline>. Published March 11, 2019.
35. ACR Appropriateness Criteria. <https://www.acr.org/Clinical-Resources/ACR-Appropriateness-Criteria>. Accessed May 20, 2019.
36. Ostlere S. How to image metal-on-metal prostheses and their complications. *AJR Am J Roentgenol* 2011;197(3):558–567.
37. Newman JS, Adler RS, Bude RO, Rubin JM. Detection of soft-tissue hyperemia: value of power Doppler sonography. *AJR Am J Roentgenol* 1994;163(2):385–389.
38. Nguyen T, Davidson BP. Contrast Enhanced Ultrasound Perfusion Imaging in Skeletal Muscle. *J Cardiovasc Imaging* 2019;27(3):163–177.
39. Palestro CJ, Love C, Miller TT. Infection and musculoskeletal conditions: Imaging of musculoskeletal infections. *Best Pract Res Clin Rheumatol* 2006;20(6):1197–1218.
40. Karchevsky M, Schweitzer ME, Morrison WB, Parellada JA. MRI findings of septic arthritis and associated osteomyelitis in adults. *AJR Am J Roentgenol* 2004;182(1):119–122.
41. Verberne SJ, Sonnegg RJA, Temmerman OPP, Raijmakers PG. What is the Accuracy of Nuclear Imaging in the Assessment of Periprosthetic Knee Infection? A Meta-analysis. *Clin Orthop Relat Res* 2017;475(5):1395–1410 [Published correction appears in *Clin Orthop Relat Res* 2017;475(6):1753–1754.].
42. Trevail C, Ravindranath-Reddy P, Sulkin T, Bartlett G. An evaluation of the role of nuclear medicine imaging in the diagnosis of periprosthetic infections of the hip. *Clin Radiol* 2016;71(3):211–219.
43. Sethi I, Baum YS, Grady EE. Current Status of Molecular Imaging of Infection: A Primer. *AJR Am J Roentgenol* 2019;213(2):300–308.